

The New Horizons Spacecraft: Past Performance, Future Potential

Christopher B. Hersman, Gabe D. Rogers, Valerie A. Mallder, Paul E. Rosendall, Brian A. Bauer, Christopher C. Deboy, Michael A. Vincent, Richard W. Webbert, Stewart S. Bushman, C. Jack Ercol, Alice F. Bowman, Karl E. Whittenburg, J. Robert Jensen, Steven R. Vernon, T. Adrian Hill, Stephen P. Williams, Carl S. Engelbrecht, and David Y. Kusnierkiewicz

ABSTRACT

On July 14, 2015, the New Horizons mission accomplished the first flyby of Pluto–Charon, achieving full mission success during its primary mission. Less than 4 years later, during its first extended mission, New Horizons flew by Arrokoth, a 36-km contact binary trans-Neptunian object in the Kuiper Belt, on January 1, 2019. Along the way, New Horizons imaged numerous distant Kuiper Belt objects, performed important heliophysics science including complex Lyman- α radiation scans, and measured the dust and zodiacal light from regions never before explored. This article provides an overview of the New Horizons spacecraft and its engineering performance, as well as potential strategies for extending the mission far beyond its original design lifetime. Details on the mass and power budgets, as well as descriptions of key innovations to meet the challenges posed by the mission, offer insight into the engineering accomplishments that led to mission success. Trended data on the power, thermal, and propulsion systems substantiate projections of the mission’s potential to continue its exploration beyond the heliopause until ~2050.

SPACECRAFT OVERVIEW

The New Horizons spacecraft was designed and developed by APL to achieve the highest-priority objective of the 2003 planetary science decadal survey: to explore Pluto and the Kuiper Belt.¹ It includes a comprehensive suite of instruments, described in detail by Fountain et al. in this issue, to address the Pluto–Kuiper Belt science objectives defined in NASA’s Pluto Kuiper Belt Mission Announcement of Opportunity (see Refs. 2 and 3 and the articles by Stern and Krimigis and Weaver et al., in this issue). Of all the mission requirements, the most formidable for the engineering team was to “arrive at Pluto as soon as possible, but not later than the 2020

timeframe.” To achieve this, the spacecraft needed to be lightweight enough to fit within the capabilities of available launch vehicles.⁴

During this period, Pluto was just beyond perihelion of 29.5 astronomical units (au) from the Sun (1 au is the distance from the Sun to Earth). As such, the solar energy was $\sim 1/1,000$ that of a spacecraft in Earth orbit, so solar arrays would not work and a radioisotope thermoelectric generator (RTG) was required. With the mass limitation imposed by the launch vehicle and the time available for development, only a single RTG could be accommodated to power the spacecraft, and no batteries for energy

storage were included. The electrical power limitations of a single RTG drove innovations to reduce peak power demands in nearly every subsystem of the spacecraft. The total power available at Pluto was predicted to be ~200 W. Finally, the need for a hibernation mode during the long-duration cruise and an encounter mode for the intensive science observation sequence during the flyby drove the design to a dual-mode guidance and control (G&C) system with spin stabilization and three-axis control. A rule-based autonomy system was developed to respond to faults and continue execution of the command sequence during critical flyby operations. Figure 1 is a block diagram of the spacecraft illustrating the various instruments and subsystems described below.

As shown in Figure 2, the compact triangular spacecraft design provides a low-mass solution for spin-balancing the spacecraft about the axis of the high-gain antenna (HGA). The placement of the RTG counterbalances the instruments and electronics. The distance between the electronics and the RTG has an added benefit of lowering the total radiation dose requirement of the electronic parts. The HGA assembly on top of the spacecraft shares the same structure for three separate antennae. The forward low-gain antenna (LGA) at the tip of the assembly provides hemispherical coverage and supports operations early in the mission. A similar LGA is positioned on the aft side of the spacecraft (not shown) to provide communications immediately

after launch. The medium-gain antenna (MGA) is the smaller dish in the middle of the assembly and is used for hibernation and safe-mode communications. The 2.1-m-diameter HGA is used for nominal operations, science data downlink, and safe modes later in the mission. The HGA features a shaped beam reflector to provide a flatter response within the pointing accuracy of the spacecraft.⁵ An important feature of the HGA is its ability to transmit both right-hand and left-hand circular polarizations simultaneously using the two traveling wave tube amplifiers (TWTAs) of the redundant radio frequency (RF) system to downlink data at nearly twice the data rate of a single polarization.⁶

Another important feature of the HGA and the communication system is the incorporation of the Radio Science Experiment (REX) into the radio receivers to minimize mass and power.⁷ In addition to REX, the New Horizons payload also includes the Alice ultraviolet (UV) imaging spectrometer,⁸ the Long Range Reconnaissance Imager (LORRI) panchromatic imager,⁹ the Ralph visible/infrared imager,¹⁰ the Solar Wind Around Pluto (SWAP) instrument,¹¹ the Pluto Energetic Particle Spectrometer Science Investigation (PEPSSI) instrument,¹² and the Venetia Burney Student Dust Counter (VSDC).¹³ The placement of the instruments on the spacecraft provides clear fields of view (FOVs) for apertures, out of the path of their thruster plumes. An overview of the New Horizons payload is provided by Weaver et al.¹⁴ and also in this issue.

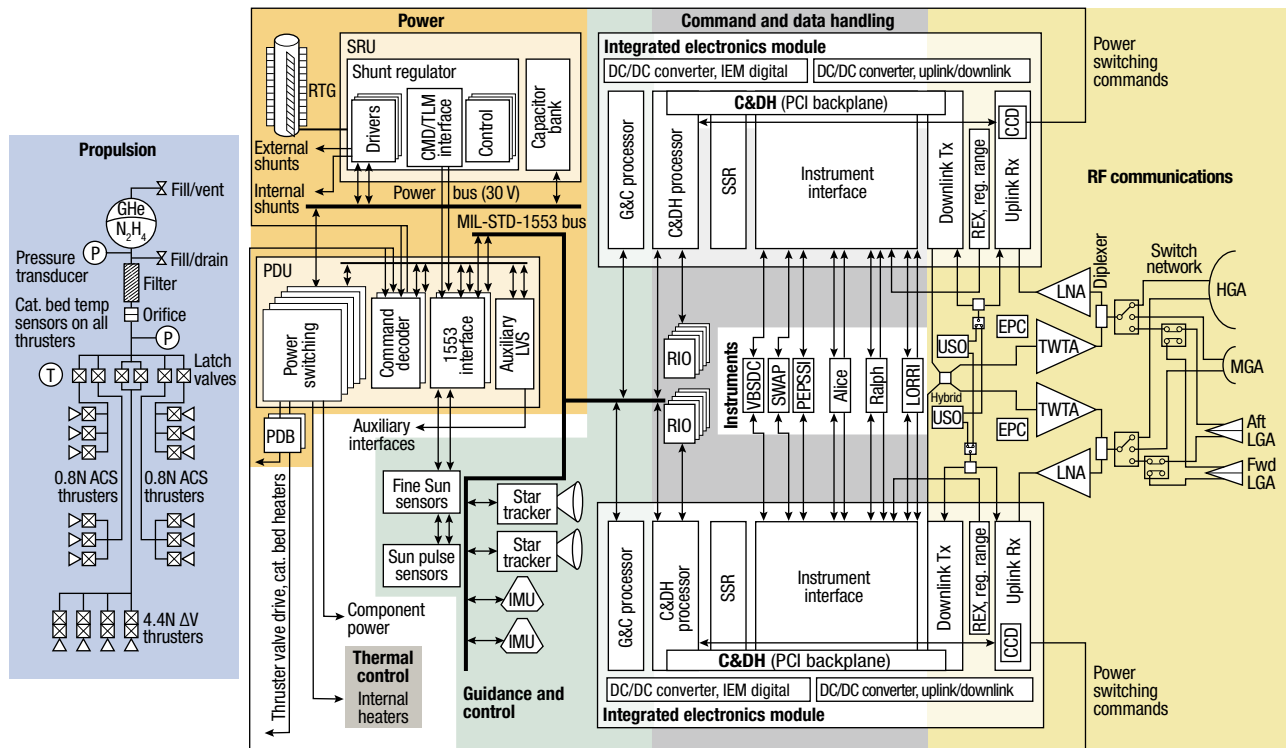


Figure 1. New Horizons block diagram. This diagram illustrates the redundancy in electronics and cross-strapping of communication interfaces.

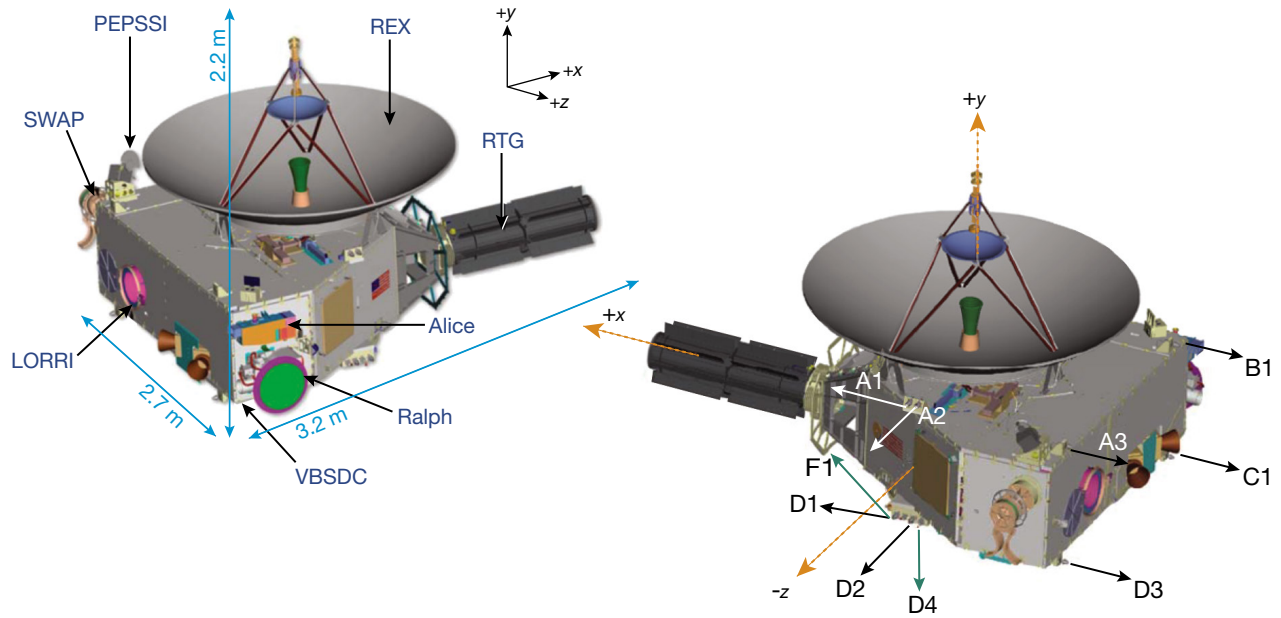


Figure 2. The overall configuration of the spacecraft showing instruments and thruster placement location of exterior components. Spacecraft dimensions in x, y, z are $10.5 \text{ ft} \times 7.3 \text{ ft} \times 9 \text{ ft}$ or $3.2 \text{ m} \times 2.2 \text{ m} \times 2.7 \text{ m}$.

In three-axis mode, the spacecraft can take images in two observation modes: scanning or staring. Figure 3 illustrates these modes, along with the sizes of the LORRI (highlighted in pink) and the Ralph (highlighted in green) FOVs. LORRI's pixel resolution is approximately four times better than Ralph's. During close flyby of a target, the Ralph imager, in a time delay integration (TDI) mode, scans wider angles, creating panoramic-like images. So that the imager clock rates can be set to match the movement of the spacecraft, the rate is communicated to the Ralph instrument onboard during the scanning observation. Simultaneous with a Ralph observation, the LORRI instrument can take high-resolution short-exposure images during scans. This capability was especially important for the Arrokoth flyby.

After each flyby, science data were downlinked using the X-band RF communication system. To reduce the power demand in the RF communication subsystems, APL developed a digital uplink receiver for the New Horizons mission. This technology development reduced the nominal power dissipation for the pair of X-band receivers to 12.9 W (Table 3), approximately half the power of comparable analog receivers.¹⁵ As mentioned previously, combining the REX and regenerative ranging capability in the New Horizons digital receiver and incorporating the redundant receivers into redundant integrated electronics modules (IEMs) saved significant mass and power and provided redundancy in the occultation observations of Pluto's atmosphere.¹⁶ The increase in receiver power when operating in REX mode is only 0.2 W per receiver.

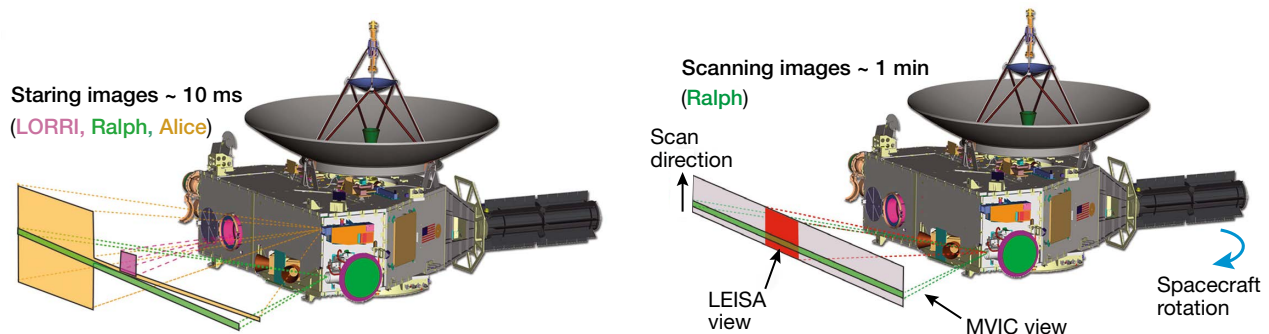


Figure 3. Spacecraft imaging modes supporting the Ralph, LORRI, and Alice instruments. The Multispectral Visible Imaging Camera (MVIC) view (green) represents the size of the visible color detector within Ralph, while the Linear Etalon Imaging Spectral Array (LEISA) view (red) represents the infrared detector within Ralph. The Alice "lollipop" field of view is shown in yellow (see the article by Fountain et al., in this issue, for more detail).

The G&C subsystems' software was constrained to use no more than two attitude control thrusters and two delta-V thrusters, simultaneously, to reduce peak power demands for active control modes. Before launch, the thruster pulse duration was tailored to provide a low minimum impulse for fine pointing stability of better than $34 \mu\text{rad/s}$. To reduce power requirements further, only one of each pair of redundant catalyst bed heaters are powered for each thruster. This approach requires the autonomy software to manage the redundancy if a catalyst bed heater fails. The thermal design for the star trackers keeps the charge-coupled device (CCD) detectors at temperatures below the threshold required for thermoelectric cooling. This reduces the operational power of the star tracker to 12.8 W. By using heat dissipation from one operating star tracker to keep the other star tracker above its survival temperature, the system does not require survival heaters unless both star trackers are powered off. Finally, the G&C software can downlink in three-axis mode with only the star tracker, so the inertial measurement unit (IMU) can be powered off to save power and preserve its operational life. In spin mode to save power, the spacecraft is placed into a passive state where the G&C processor, star tracker, IMU, and Sun sensors can all be off while the spacecraft is downlinking data.

Substantial flexibility has been designed into the G&C subsystem. Many capabilities have been essential to mission success, while others have yet to be used but may enable mission extensions long beyond the spacecraft's design life. For example, beyond the standard pointing modes, the G&C software is also equipped with a relative control mode. This mode uses the high-rate IMU data to actively control the inertial stability to within $20 \mu\text{rad}$ (a single 4×4 -binned pixel of the LORRI instrument) for up to 60 s. On approach to Arrokoth, relative control mode was essential for optical navigation. The thrusters are an example of a capability that will be essential in extending the mission life. The system was built to be able to control the spacecraft with a subset of thrusters if one fails. Although all thrusters are fully operational, eventually the available power will no longer support the use of all 12 catalyst bed heaters at the same time. Since the control algorithms can operate in a three-axis mode with half the required thrusters (or even fewer in a spinning mode), the mission can continue to operate at a reduced power level. More details are in the section on future potential.

In the thermal design, the power constraints dictated that no operational heaters would be used in peak science modes during the Pluto flyby. Waste heat from the RTG and onboard electrical components is used to maintain the spacecraft temperatures. The thermal subsystem was designed to minimize thermal leaks, which resulted in the internal temperature of the spacecraft being tightly coupled to the internal power dissipation. Louvers allow

heat from the higher-power components to be radiated when those devices are warm.¹⁷ Flight software manages the overall spacecraft temperature using thermal control algorithms to determine when operational heaters are needed.¹⁸ This implementation has resulted in a propellant tank temperature that has remained above 14°C for the past 16 years and can be maintained at an appropriate operating level for many years to come, as described in more detail in the section on future potential.

The power subsystem includes features to support other subsystem capabilities. A large 33-mF capacitor bank provides additional energy for turn-on transients and momentary switching events. The power distribution unit (PDU) enforces a time delay between the powering on of multiple spacecraft components to prevent simultaneous turn-on transients. A critical "hold-off" feature allows redundant sides of critical components, such as receivers, command and data handling (C&DH) processors, and power subsystem interfaces, to be powered off. If the primary C&DH processor fails to maintain communication with the power subsystem, all redundant critical components are powered on and the autonomy system reconfigures the spacecraft. The shunt regulator unit can switch some of the external shunts to internal heaters to provide more heat inside the spacecraft later in the mission. This feature is integral to the thermal subsystem and thermal control software.

The C&DH processor operates at 12 MHz to reduce the power demands of this subsystem. APL also built a 64-Gbit flash memory solid-state recorder (SSR), which provided substantial power savings over random access memory (RAM) recorders. Because the memory retains its data while powered off, the recorder was designed to power only the parts being accessed. The total power requirement for the primary C&DH subsystem is 9.1 W, including the SSR and instrument data interfaces.

The C&DH processor software provides the fault management capability known as the autonomy system to respond to spacecraft events by executing various command sequences. The autonomy system has been programmed with ~ 170 predefined rules that maintain the safety of the system in the event of anomalies. The autonomy system also transitions to safe modes (described below) and enforces encounter mode.¹⁹ Spacecraft modes are shown in Figure 4.

The spacecraft modes include autonomous transition from operational modes (in green) to safe modes (e.g., Earth acquisition, Sun acquisition; in red) in the event of a critical fault. The primary purpose of these safe modes is to maintain the safety of the spacecraft and configure the spacecraft for communication with the ground. In the case of three-axis encounter mode, the spacecraft is programmed to autonomously address all faults and continue the critical encounter sequence. Only after exiting encounter mode can the spacecraft enter a safe mode. If the encounter exit command is

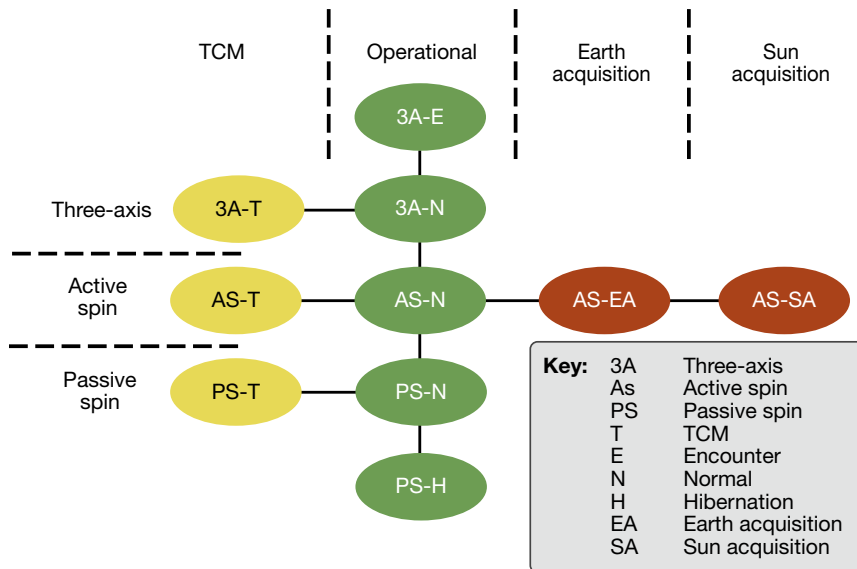


Figure 4. Spacecraft modes. This diagram shows the paths for autonomous transitions from trajectory correction maneuver (TCM) (yellow) and operational modes (green) to safe modes (red). For three-axis encounter mode (3A-E), autonomous transitions to safe modes are only permitted after a preset timeout.

not executed as planned, the encounter mode timeout occurs and the spacecraft then transitions to a safe mode. In case the spacecraft were to transition to safe mode just prior to a scheduled encounter mode entry, a Stream-Lined Autonomy Macro (SLAM) was developed to enable the mission operations team to enter encounter mode quickly and jump to the current time in the command sequence using a single procedure.

In addition to fault management, the C&DH flight software controls the uplink and downlink functionality and implements SSR recording, compression, and playback of instrument science data and spacecraft house-keeping telemetry. The C&DH flight software manages the communication between subsystems and components on the spacecraft.

Other innovations on New Horizons were implemented by partner organizations. For example, the Sector Microwave Single-Pole, Triple-Throw RF switches were modified to reduce the peak power required for operation. The Adcole (now Redwire Space) Sun sensors, used for active spin-Sun acquisition safe mode, incorporated an adjustable gain setting with seven range settings because of the large dynamic range of the sunlight between 1 and 50 au.²⁰ The Honeywell miniature IMU gyros were hand-selected using preliminary test data to maximize the predicted lifetime. The Galileo Autonomous Star Tracker software was modified to add a spinning capability to the existing heritage three-axis star tracker without changing the flight-qualified hardware.²¹ Spacecraft spinning mode was necessary for hibernation, which reduced risk and operational cost during the 9-year cruise to Pluto and the subsequent journey through the Kuiper Belt.²²

This long cruise to Pluto influenced the reliability requirements of the design. Every effort was made to minimize the use of mechanisms. When instrument covers were required for launch, they were deployed early in the mission. Usage of life-limited items, such as thruster cycles and IMU operational hours, is tracked throughout the mission. Where possible, redundancy and cross-strapped interfaces were used to increase reliability, as illustrated in Figure 1. For example, the RF communication subsystem provides the capability to connect either uplink receiver to any of the antennae, as well as downlink via either TWTA from either side. The MIL-STD-1553²³ bus provides communication from the primary C&DH processor (bus controller) to other components of the spacecraft (remote terminals). The

backup C&DH processors can play back data from the backup SSR directly via RF downlink or via the primary C&DH bus controller. The systems are designed to be single-fault tolerant with a few exceptions (e.g., the RTG, propellant tank, RF hybrid, and HGA structure).

The uplink and downlink boards within the integrated electronics module make up the RF communications transceiver. The low-power transceiver is an alternative to a deep-space transponder and is critical to meeting the spacecraft power budget. The ultra-stable oscillator (USO) provides the precise frequency reference needed for uplink radio science. The RF subsystem is used for command and telemetry, range/Doppler tracking, and the uplink REX.

The spacecraft mass budget is shown in Table 1. The total mass allocated to instruments is 32.7 kg, ~7% of the overall launch mass of the system. The total wet mass of 478.1 kg achieved the requirement for a lift mass of <478.5 kg.

Power modes for the instruments and spacecraft are shown in Tables 2 and 3, respectively. The modes include those currently used in spacecraft operation and those that could be used in the future to reduce the power requirements onboard the spacecraft and extend the mission lifetime. These modes are discussed in more detail in the final section of this article. The spacecraft power budget allocates 15 W for all transient operational modes (see Table 3). Timing of transients is constrained such that they do not occur simultaneously. Transients >15 W were scheduled to occur early in the mission when the RTG power output was higher or other components were not powered.

Table 1. Spacecraft mass budget

	Source	Units	Unit Mass (kg)	Total Mass (kg)
Instruments				32.7
Alice	Southwest Research Institute (SwRI)	1	4.5	4.5
Ralph	SwRI, Ball Aerospace	1	10.3	10.3
LORRI	APL, SSG	1	8.8	8.8
SWAP	SwRI	1	3.3	3.3
PEPSSI	APL	1	1.5	1.5
VBSDC	Laboratory for Atmospheric and Space Physics (LASP)	1	1.9	1.9
REX (mass included in IEM)	Stanford, APL	2	—	—
Instrument support structure	APL	1	2.4	2.4
RF Communications				38.8
Antenna assemblies (HGA, MGA, LGAs)	APL	1	19.8	19.8
TWTA, electronic power conditioner	Thales	2	2.5	5.0
USO	APL	2	1.2	2.5
Oscillator switch assembly	APL	2	0.2	0.5
RF switch network assembly	APL	2	3.6	7.2
Waveguides, coax	APL	1	3.8	3.8
IEM				23.3
Assembly	APL	2	11.4	22.8
Remote input output units	APL	14	0.0	0.5
Power				86.2
RTG	Department of Energy	1	57.8	57.8
PDU	APL	1	18.3	18.3
Shunt regulator unit (SRU)	APL	1	8.1	8.1
Shunt dissipators	APL	2	1.0	2.0
Structure				124.4
Balance mass	APL	1	27.0	27.0
Primary and secondary structure, purge system	APL, Canyon, Swales	1	97.3	97.3
Guidance and Control				19.5
Sun sensors	Adcole	1	1.7	1.7
Star tracker	Galileo Avionica	2	3.2	6.4
Star tracker bracket	APL	1	1.7	1.7
IMU	Honeywell	2	4.9	9.7
Thermal				27.8
IMU louvers	Starsys	2	0.7	1.4
IEM louvers	Starsys	2	0.9	1.9
Multilayer insulation	APL	1	15.3	15.3
Micrometeoroid protection	APL	1	7.3	7.3
Miscellaneous (sensors, thermostats)	APL	1	2.0	2.0
Propulsion				28.0
Propulsion hardware (tank, valves, filters)	Aerojet Rocketdyne	1	24.9	24.9
Propulsion diode box	Swales Aerospace	2	1.6	3.1
Harness				20.6
Harness	APL	1	19.7	19.7
Miscellaneous (tie-downs, lacing, brackets)	APL	1	1.0	1.0
Total dry mass				401.3
Propellant, pressurant	Kennedy Space Center			76.8
Total mass				478.1^a

^aMargin was used to add more propellant to reach to total mass of 478.1 kg.

Table 2. Power constraints required selected instruments to be powered depending on the type of science activity

	Units	Unit Power (W)	Current			Future
			Pluto Imaging Science	Pluto Atmosphere Science	Arrokoth Imaging Science	Low-Power Helio Science
Total			194.6	182.2	184.8	69.9
Instruments			27.4	15.0	17.6	9.9
Alice	1	4.7	4.7	4.7		
Ralph	1	7.1	7.1		7.1	
LORRI	1	5.8	5.8		5.8	
SWAP	1	2.3	2.3	2.3	2.3	2.3
PEPSSI	1	2.5	2.5	2.5	2.5	2.5
VBSDC	1	5.0	5.0	5.0		5.0
REX	2	0.2		0.4		
Spacecraft			167.2	167.2	167.2	60.1
Spacecraft Mode			3A-E Science 2CDH	3A-E Science 2CDH	3A-E Science 2CDH	PS-N Low Power

PAST PERFORMANCE

This section highlights how the spacecraft performed in the face of technical challenges during the Pluto flyby on July 14, 2015, and the Arrokoth flyby on January 1, 2019. During the Pluto flyby, the spacecraft used a special tracking mode to vary its attitude maneuver rate to match the flyby geometry such that the TDI imaging line rate remained constant from the perspective of the Ralph instrument. This approach minimized the pixel smear in the Ralph TDI panoramic image shown in Figure 5, highlighting distinct layers in Pluto's atmosphere and topographical features on its surface.

During the Arrokoth flyby, the science operations, navigation, and G&C teams worked closely to obtain

the highest-resolution images possible by precisely targeting the flyby trajectory and nearly filling the entire LORRI field with Arrokoth, while the Ralph imager scanned the entire region of uncertainty. (See the article by Holdridge et al., in this issue, for more on encounter design, planning, and navigation.) LORRI took over 900 images during this Ralph scan, 9 of which contained Arrokoth. These 9 LORRI images are shown in sequence in Figure 6, with the FOV outlined in pink. By combining these data with color images from Ralph, the composite image of Arrokoth shown in Figure 7 was produced and featured on the cover of *Science* magazine.

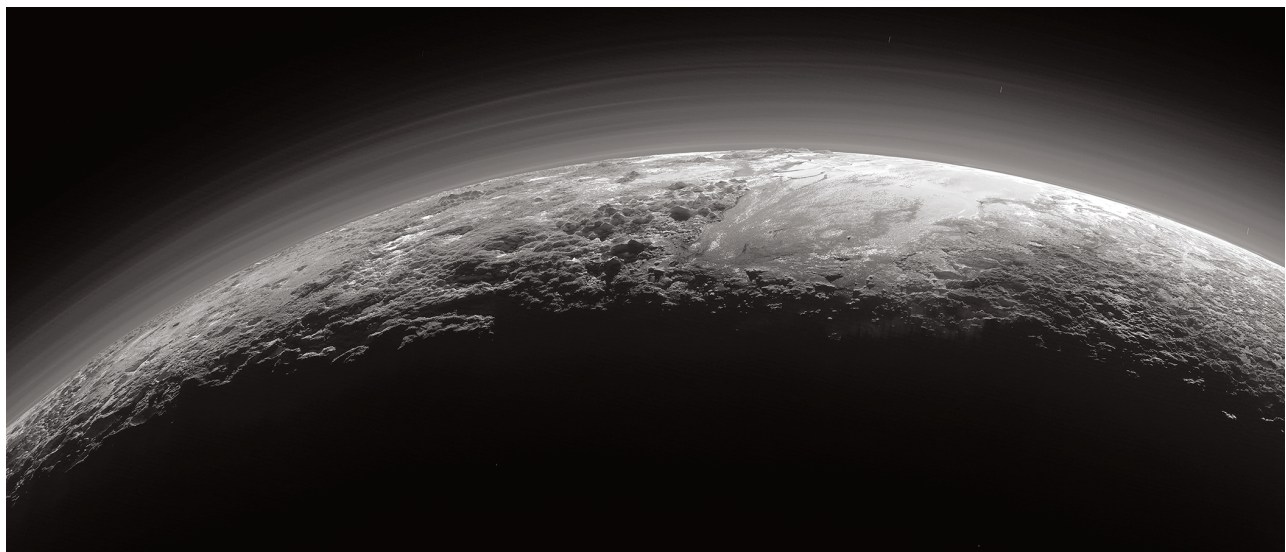


Figure 5. Panoramic image of Pluto. The image was obtained using Ralph's TDI scanning mode and a special G&C tracking mode.

Table 3. Careful tracking of power allocations for all spacecraft modes is essential to ensure adequate power during flight

Spacecraft Power By Mode	Units	Unit Power (W)	Current										Future					
			AS-EA		3A-E		3A-TCM		3A-N		3-Axis 2CDH		AS-N Low		AS-N Low		PS-N Low	
			PS-N ITWTA	AS-N ITWTA	2CDH	3A-TCM	Pre-TCM	ITWTA	2TWTA	warm-up	Power thrusting	ITWTA	Power	ITWTA	Power			
RF Communications			109.6	158.3	167.2	186.6	176.2	168.0	151.5	109.3	109.7	100.6	60.1					
Uplink receiver	2	6.5	57.4	57.4	25.2	25.2	25.2	57.4	89.6	8.9	8.9	48.6	8.9					
Downlink transmitter	2	7.5	12.9	12.9	12.9	12.9	12.9	12.9	12.9	6.5	6.5	6.5	6.5					
TWTA	2	32.2	32.2	32.2	32.2	32.2	32.2	32.2	64.4	7.5	7.5	32.2	7.5					
USO	2	2.4	4.8	4.8	4.8	4.8	4.8	4.8	4.8	2.4	2.4	2.4	2.4					
IEM			9.1	9.1	18.0	18.0	18.0	18.0	18.0	9.1	9.1	9.1	9.1					
C&DH processor 1, interface card, remote input/output units, and SSR	1	9.1	9.1	9.1	9.1	9.1	9.1	9.1	9.1	9.1	9.1	9.1	9.1					
C&DH processor 2, interface card, remote input/output units, and SSR	1	8.9	8.9	8.9	8.9	8.9	8.9	8.9	8.9	8.9	8.9	8.9	8.9					
Power			17.2	17.2	17.2	17.2	17.2	17.2	17.2	17.2	17.2	17.2	17.2					
PDU command decoders	2	2.5	5.0	5.0	5.0	5.0	5.0	5.0	5.0	5.0	5.0	5.0	5.0					
PDU telemetry, 1553 interface	2	4.5	4.5	4.5	4.5	4.5	4.5	4.5	4.5	4.5	4.5	4.5	4.5					
Unswitched PDU dissipation	1	3.3	3.3	3.3	3.3	3.3	3.3	3.3	3.3	3.3	3.3	3.3	3.3					
SRU telemetry	2	1.6	1.6	1.6	1.6	1.6	1.6	1.6	1.6	1.6	1.6	1.6	1.6					
Unswitched SRU dissipation	1	2.8	2.8	2.8	2.8	2.8	2.8	2.8	2.8	2.8	2.8	2.8	2.8					
G&C			8.7	21.1	52.5	52.5	52.5	21.1	8.7	52.5	48.5	8.7	8.7					
G&C processor	2	8.4	8.4	8.4	8.4	8.4	8.4	8.4	8.4	8.4	8.4	8.4	8.4					
Sun sensor (for safing only)	2	2.1	2.1	2.1	2.1	2.1	2.1	2.1	2.1	2.1	2.1	2.1	2.1					
Star tracker	2	12.8	12.8	12.8	12.8	12.8	12.8	12.8	12.8	12.8	12.8	12.8	12.8					
Star tracker heater	2	8.7	8.7	8.7	8.7	8.7	8.7	8.7	8.7	8.7	8.7	8.7	8.7					
IMU	2	31.4	31.4	31.4	31.4	31.4	31.4	31.4	31.4	31.4	31.4	31.4	31.4					
Propulsion			0.0	35.3	35.9	54.9	44.7	35.9	0.0	4.4	8.9	0.0	0.0					
Attitude control thruster	12	4.4	8.9	8.9	8.9	8.9	8.9	8.9	8.9	4.4	8.9	0.0	0.0					
Attitude control thruster catalyst bed heater	24	2.2	26.4	26.4	26.4	26.4	26.4	26.4	26.4	4.4	8.9	0.0	0.0					
Delta velocity thruster	4	9.5	19.0	19.0	19.0	19.0	19.0	19.0	19.0	4.4	8.9	0.0	0.0					
Delta velocity thruster catalyst bed heater	8	2.2	8.8	8.8	8.8	8.8	8.8	8.8	8.8	4.4	8.9	0.0	0.0					
Pressure transducer	2	0.7	0.7	0.7	0.7	0.7	0.7	0.7	0.7	0.7	0.7	0.7	0.7					
Transient Allocation			15.0	15.0	15.0	15.0	15.0	15.0	15.0	15.0	15.0	15.0	15.0					
15 W transient allocation	1	15.0	15.0	15.0	15.0	15.0	15.0	15.0	15.0	15.0	15.0	15.0	15.0					
Harness			2.2	3.2	3.3	3.7	3.5	3.4	3.0	2.2	2.2	2.0	1.2					
Harness losses (2% of total power)	1	2.2	3.2	3.3	3.7	3.5	3.4	3.0	2.2	2.2	2.0	1.2	1.2					

Overall, component power dissipations on the spacecraft have remained constant throughout the mission.

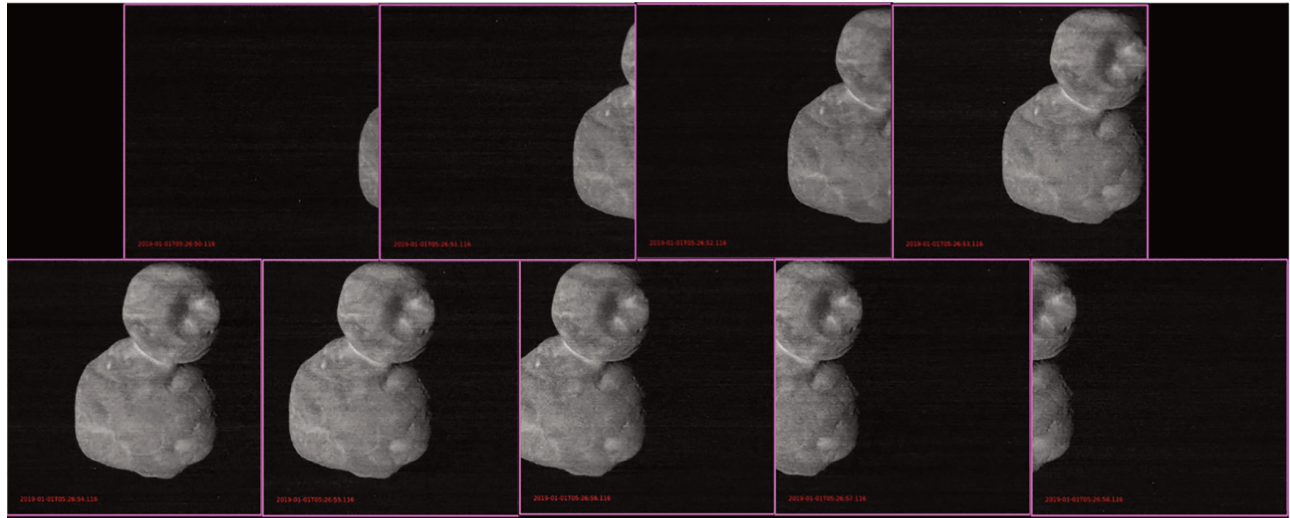


Figure 6. The LORRI instrument’s sequence of high-resolution snapshots. While the Ralph instrument scanned the entire region of uncertainty during the Arrokoth flyby, LORRI took over 900 images. These nine images contain the highest-resolution data from the flyby. The LORRI FOV is outlined in pink in each frame, and a time stamp has been added in red.



Figure 7. Composite image of Arrokoth. LORRI images were combined with color images from Ralph to create the composite image of Arrokoth. It was featured on the cover of *Science* magazine.

Power Performance

The RTG power output is trending as expected. The approximate rate of decay in power output is currently about 3.2 W/year. The power output since launch is shown as a bold blue line in Figure 8, along with an estimated projection of predicted performance beyond 2022. When planning future activities, the power margin is calculated by subtracting the peak power demand during the planned activity from this projected estimate of RTG power output. When command sequences are

developed, a software simulation tool is used to verify that the activities do not exceed the predicted onboard power available.

Thermal Performance

The thermal subsystem’s performance has been stable. Overall temperatures are gradually cooling as expected. All components remain well within their specified operational ranges. As an example, Figure 9 shows the

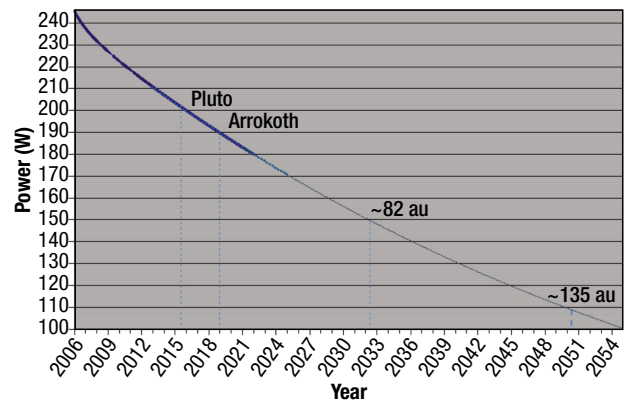


Figure 8. RTG power output. Power output is trending as expected, with the current decay rate at ~3.2 W/year. The labels for Pluto and Arrokoth show the power that was available during the flybys. The ~82 au and ~135 au labels show the distance of the spacecraft from the Sun when the output reaches 150 W and 110 W, respectively. These milestones represent the expected capability of the current spacecraft without modification (which requires 150 W) and the expected power required to actively control the spacecraft with updates to the G&C and autonomy systems (which requires only 110 W). For more information, see Whiting and Woerner.²⁴

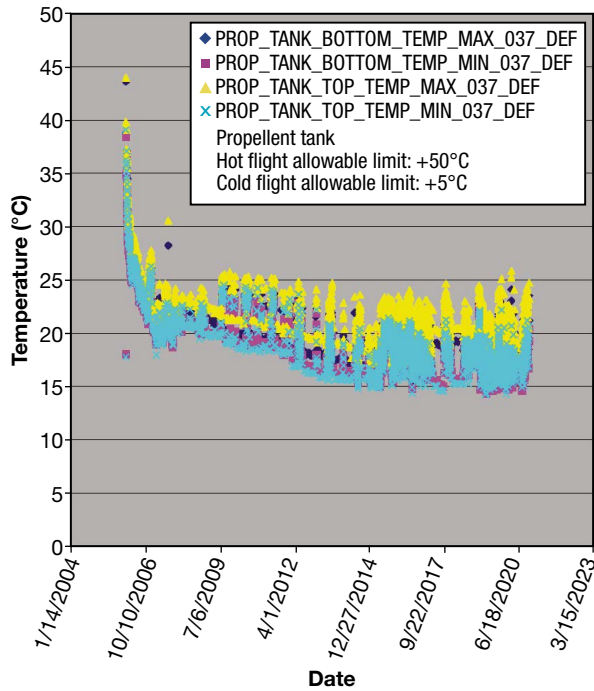


Figure 9. Propellant tank temperature since launch. Temperatures are gradually cooling as expected, remaining above 14°C, well above the freezing point of hydrazine.

maximum and minimum propellant tank temperatures since launch; they have remained above 14°C, well above the freezing point of hydrazine.

G&C Performance

The G&C subsystem’s performance has exceeded requirements. The pointing requirements and performance are shown in Table 4.

The spacecraft’s ability to spend most of its time in spin mode preserves the operational lifetime of the IMUs. As of 2022, the spacecraft has been operating for nearly 150,000 h since launch, but the combined operational hours of the IMUs has only been ~30,000 h (~20% of the time).

Propulsion Performance

The amount of propellant budgeted for New Horizons provided the ability to correct launch injection errors of up to 3-sigma. Since the Atlas V 551 provided exceptional launch accuracy, the propellant allocated for

Table 4. G&C requirements and performance

G&C Parameter	Requirement (μrad)	Performance (μrad)
Pointing control	±1024	±600
Pointing knowledge	±471	±200
Relative control mode	±20 for 10 s	±20 for >10 s

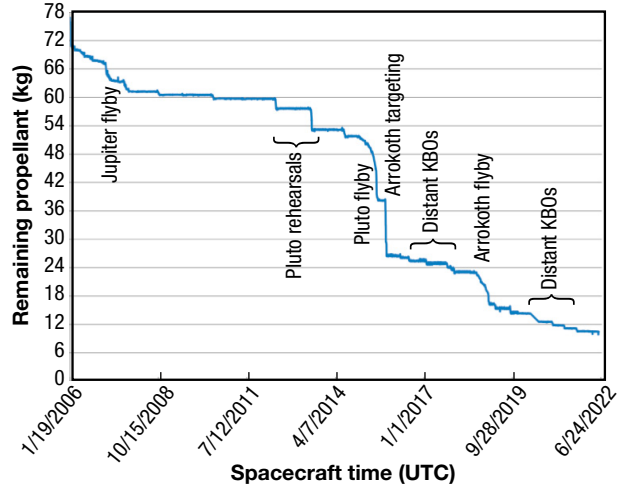


Figure 10. Propellant use as a function of time.

correcting launch injection errors was available for the extended mission. This additional propellant increased the probability that a Kuiper Belt object would be within the reach of the spacecraft’s trajectory. Figure 10 shows the propellant usage as a function of time. The most significant uses of propellant occurred during the initial launch correction, Jupiter flyby, Pluto rehearsals, Pluto flyby, Arrokoth targeting maneuver, and Arrokoth flyby.

RF Communications Performance

The RF performance has exceeded requirements. Downlink data rates as a function of time are shown in Figure 11. USO stability is shown in Figure 12 and Table 5.

C&DH Performance

During both the Pluto and Arrokoth flybys, both redundant C&DH processors (each with a separate

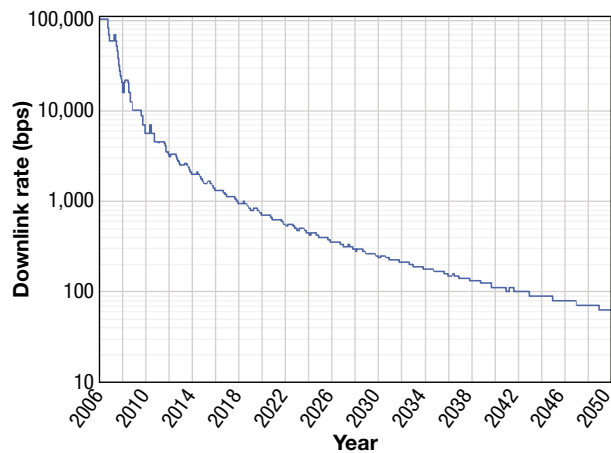


Figure 11. Downlink rates as a function of time for a single TWTA to a Deep Space Network 70-m ground antenna. If power is sufficient to use both TWTAs, the data rates nearly double.

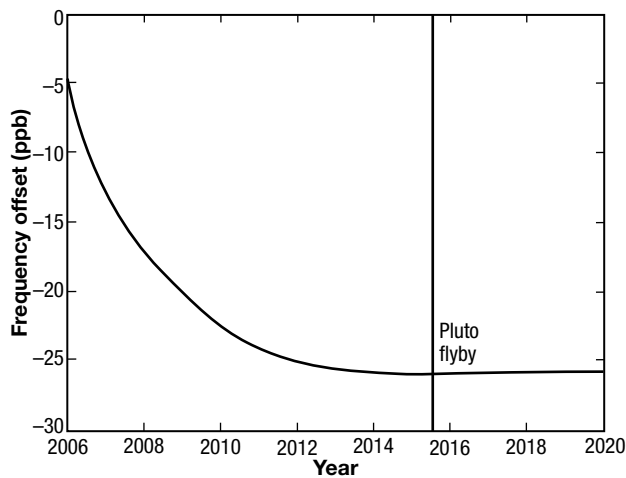


Figure 12. USO stability. The stability of the USO achieving a few parts per billion was critical to the REX observations of Pluto's atmosphere, and the best stability was achieved during the Pluto flyby.

Table 5. REX frequency stability requirements for the New Horizons USO

Interval (s)	δ/f
0.1–1.0	1×10^{-12}
1.0–10	3×10^{-13}
10–100	3×10^{-13}

SSR) gathered extra data and at higher recording rates (compared with a single SSR). The C&DH subsystem offers the flexibility to record two instruments to different SSRs or the same instrument simultaneously on both SSRs. As explained above, during the Arrokoth flyby, LORRI high-resolution panchromatic images were recorded to one SSR while Ralph high-rate TDI panoramic scans were simultaneously recorded to the other. Without the use of both SSRs, the combined data rate would have exceeded the recording rate of a single SSR. During both flybys, the highest-priority observations, which were critical for mission success, were recorded redundantly. The redundant data ensured that the loss of a single C&DH processor or SSR would not jeopardize mission success. For Pluto, ~20 Gbit of the flyby data were recorded redundantly and ~20 Gbit were unique on each SSR. This approach enabled New Horizons to gather a total of ~60 Gbit of science data using both C&DH processors and SSRs, far exceeding the original requirement of 10.2 Gbit.

One operational complication related to C&DH performance has been the number of C&DH processor resets. Although C&DH processor resets were predicted, the in-flight experience of ~1/year is ~10 times more than prelaunch estimates. The root cause of some processor resets was traced to a software coding error that has since been corrected. Others, however, are the result

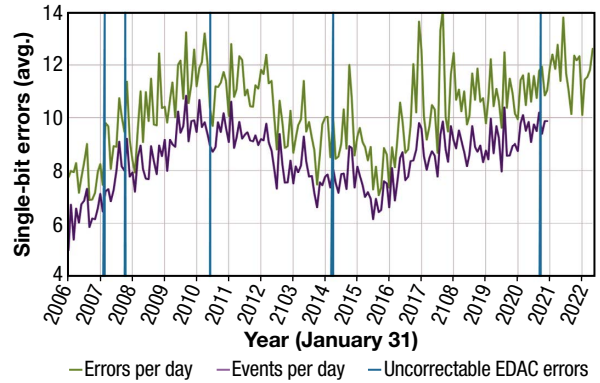


Figure 13. Monthly average single-bit errors per day in C&DH static RAM. After 2020 we no longer distinguish between errors and events (bursts of errors). We continue to trend individual errors.

of radiation-induced effects and cannot be eliminated. Single-bit errors in memory are correctable using processors' error detection and correction circuits (EDAC). Two errors in the same memory location are detectable, but not correctable, and result in a reset of the processor. The radiation events are often correlated, such that a single event results in multiple errors in separate locations in memory. The number of events and the number of single errors in memory are reflected in the two plots (purple and green, respectively) in Figure 13. The blue lines indicate uncorrectable EDAC errors.

FUTURE POTENTIAL

As of June 2023, all systems onboard the New Horizons spacecraft are nominal, and telemetry is trending as expected. Careful management and monitoring of onboard consumable resources, such as power, propellant, thruster cycles, and operational hours, has positioned New Horizons with the potential to continue exploring the solar system for decades.

Trending

Data have been trended to predict available resources as a function of time, such as RTG power output, onboard temperatures, and downlink data rates. Methods have been identified to reduce resource demands, such as power dissipation and propellant use. Budgets have been used to predict the expected lifetime of limited-life items, such as thruster cycles and IMU operational hours. Finally, contingency plans have been developed to respond if issues arise.

At this phase of the mission, with the spacecraft in a spin-stabilized attitude, New Horizons can maintain communication with Earth for ~100 days/year without any attitude maneuvers. Provided the spacecraft hibernates for the remaining 265 days, its operations could be

limited to a single attitude precession each year, using only ~10 g of propellant per year. This approach has an added benefit: if the ability to precess were lost, such as might be the case if the propellant freezes, the spacecraft could continue communicating with Earth for an additional 7 years without any attitude changes.

Power

One method for extending spacecraft lifetime is to develop new operational techniques to minimize the peak power demands of the spacecraft. An example is powering only a subset of the 24 thruster catalyst bed heaters. Currently, one catalyst bed heater is powered for each of the 12 thrusters. In the future, it may be possible to sequence operations to require only two catalyst bed heaters to be powered at the same time. Each catalyst bed heater requires 2.2 W and the average decrease of the RTG power is 3.2 W/year, so saving 10 catalyst bed heaters could extend the mission by almost 7 years. Based on the power analysis shown in Table 2, the “Low Power Downlink 1TWTA” capability would be usable until ~2050.

Thermal

Consistent with the power predictions, the thermal trending shown in Figure 14 indicates that the tank temperature may remain above the freezing temperature of hydrazine until ~2050.

G&C and Propulsion

In the spinning-mode operations concept of 100 days of active operations per year, the demands on the G&C and propulsion systems are minimal. A single precession per year minimizes the thruster cycles, propellant use, and IMU operational hours. With this approach, none of these G&C resources is expected to limit the life of the New Horizons mission.

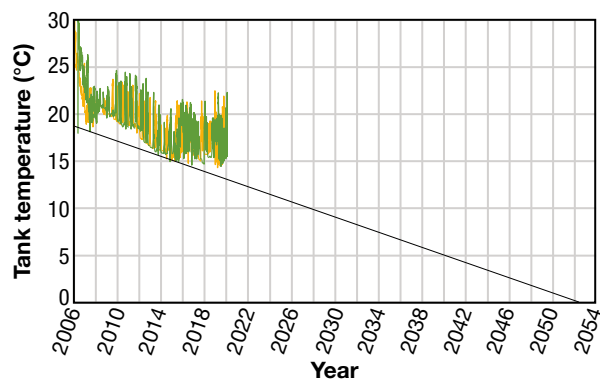


Figure 14. Projected thermal trending of the minimum propellant tank temperature. The tank temperature may remain above the freezing temperature of hydrazine until ~2050.

C&DH and RF Communications

In ~2050, uplink command rates of 125 bps and downlink data rates of ~50 bps are expected, as shown Figure 11. TWTA operational hours are trending as predicted, so the TWTAs are not expected to be a concern for the mission lifetime. There are no other life-limiting aspects to the C&DH or RF communications subsystems.

CONCLUSION

After successfully completing its primary mission to Pluto and its first extended mission to Arrokoth, a Kuiper Belt object, New Horizons is on course to continue exploring the solar system and beyond. With careful management of the spacecraft resources and continued good fortune, the lifetime of the New Horizons spacecraft is anticipated to extend until ~2050 and to a distance of ~135 au from the Sun.

ACKNOWLEDGMENTS: Work on the New Horizons mission was performed under NASA contracts NAS5-97271/TO30 (APL) and NASW-02008 (SwRI).

REFERENCES

- ¹National Research Council, *New Frontiers in Solar System Exploration*. Washington, DC: National Academies Press, 2003, <https://doi.org/10.17226/10898>.
- ²NASA, “Pluto Kuiper Belt mission announcement of opportunity,” AO 01-OSS-01, Jan. 19, 2001.
- ³S. A. Stern, “The New Horizons Pluto Kuiper Belt mission: An overview with historical context,” *Space Sci. Rev.*, vol. 140, pp. 3-21, 2008, <https://doi.org/10.1007/s11214-007-9295-y>.
- ⁴Y. Guo and R. W. Farquhar, “New Horizons mission design,” *Space Sci. Rev.*, vol. 140, pp. 49-74, 2007, <https://doi.org/10.1007/s11214-007-9242-y>.
- ⁵R. Schulze and S. Hill, “The New Horizons high gain antenna: Reflector design for a spin-stabilized bus at cryogenic temperatures,” in *Proc. 2004 IEEE Aerosp. Conf.* (IEEE Cat. No.04TH8720), vol. 2, pp. 966-974, 2004, <https://doi.org/10.1109/AERO.2004.1367697>.
- ⁶T. Pham and C. DeBoy, “Polarization combining in the DSN - Recent results,” in *IEEE MTT-S Int. Microwave Symp. Dig.*, pp. 943-946, 2007, <https://doi.org/10.1109/MWSYM.2007.380173>.
- ⁷G. L. Tyler, I. R. Linscott, M. K. Bird, D. P. Hinson, D. F. Strobel, et al., “The New Horizons Radio Science Experiment (REX),” *Space Sci. Rev.*, vol. 140, pp. 217-259, 2008, <https://doi.org/10.1007/s11214-007-9302-3>.
- ⁸S. A. Stern, D. C. Slater, J. Scherrer, J. Stone, G. Dirks, et al., “ALICE: The ultraviolet imaging spectrograph aboard the New Horizons Pluto-Kuiper Belt mission,” *Space Sci. Rev.*, vol. 140, art. 155, 2008, <https://doi.org/10.1007/s11214-008-9407-3>.
- ⁹A. F. Cheng, H. A. Weaver, S. J. Conard, M. F. Morgan, O. Barnouin-Jha, et al., “Long-Range Reconnaissance Imager on New Horizons,” *Space Sci. Rev.*, vol. 140, pp. 189-215, 2008, <https://doi.org/10.1007/s11214-007-9271-6>.
- ¹⁰D. C. Reuter, S. A. Stern, J. Scherrer, D. E. Jennings, J. W. Baer, et al., “Ralph: A visible/infrared imager for the New Horizons Pluto/Kuiper Belt mission,” *Space Sci. Rev.*, vol. 140, pp. 129-154, 2008, <https://doi.org/10.1007/s11214-008-9375-7>.
- ¹¹D. McComas, F. Allegrini, F. Bagenal, P. Casey, P. Delamere, et al., “The Solar Wind Around Pluto (SWAP) Instrument aboard New Horizons,” *Space Sci. Rev.*, vol. 140, pp. 261-313, 2008, <https://doi.org/10.1007/s11214-007-9205-3>.

- ¹²R. L. McNutt Jr., S. A. Livi, R. S. Gurnee, M. E. Hill, K. A. Cooper, et al., “The Pluto Energetic Particle Spectrometer Science Investigation (PEPSSI) on the New Horizons mission,” *Space Sci. Rev.*, vol. 140, pp. 315–385, 2008, <https://doi.org/10.1007/s11214-008-9436-y>.
- ¹³M. Horányi, V. Hoxie, D. James, A. Poppe, C. Bryant, et al., “The Student Dust Counter on the New Horizons mission,” *Space Sci. Rev.*, vol. 140, pp. 387–402, <https://doi.org/10.1007/s11214-007-9250-y>.
- ¹⁴H. A. Weaver, W. C. Gibson, M. B. Tapley, L. A. Young, and S. A. Stern, “Overview of the New Horizons science payload,” *Space Sci. Rev.*, vol. 140, pp. 75–91, 2008, <https://doi.org/10.1007/s11214-008-9376-6>.
- ¹⁵C. B. Haskins and W. P. Millard, “X-band digital receiver for the New Horizons spacecraft,” in *Proc. 2004 IEEE Aerospace Conf. (IEEE Cat. No.04TH8720)*, vol. 3, pp. 1479–1488, 2004, <https://doi.org/10.1109/AERO.2004.1367923>.
- ¹⁶C. C. Deboy, C. Haskins, D. Duven, R. Schulze, J. R. Jensen, M. Bernacik, and W. Millard, “The New Horizons mission to Pluto: Advances in telecommunications system design,” *Acta Astronautica*, vol. 57, pp. 540–553, 2005, <https://doi.org/10.1016/j.actaastro.2005.03.051>.
- ¹⁷G. H. Fountain, D. Y. Kusnierkiewicz, C. B. Hersman, T. S. Herder, T. B. Coughlin, et al., “The New Horizons spacecraft,” *Space Sci. Rev.*, vol. 140, pp. 23–47, 2008, <https://doi.org/10.1007/s11214-008-9374-8>.
- ¹⁸E. Birrane, S. Williams, and D. Mehoke, “Software controlled thermal power management on New Horizons,” *Space 2006*, AIAA-2006-7289, 2006, <https://doi.org/10.2514/6.2006-7289>.
- ¹⁹R. C. Moore, “Autonomous safeing and fault protection for the New Horizons mission to Pluto,” in *Proc. 57th Int. Astronaut. Cong., IAC-06-D1.4.07*, 2006, <https://doi.org/10.2514/6.IAC-06-D1.4.07>.
- ²⁰G. D. Rogers, M. Schwinger, H. Ambrose, and J. Kaidy, “New Horizons guidance and control system performance during early operations,” in *Proc. AIAA Guid. Navigation Control Conf. and Exhib.*, AIAA 2007-6729, 2007, <https://doi.org/10.2514/6.2007-6729>.
- ²¹G. D. Rogers, M. R. Schwinger, J. T. Kaidy, T. E. Strikwerda, R. Casini, et al., “Autonomous star tracker performance,” in *Proc. 57th Int. Astronaut. Cong., IAC-06-D1.2.01*, <https://doi.org/10.2514/6.IAC-06-D1.2.01>.
- ²²A. Bowman, “Spacecraft hibernation: Concept vs. reality, a mission operations manager’s perspective,” in *Proc. AIAA SpaceOps 2010 Conf.*, AIAA 2010-2161, 2010, <https://doi.org/10.2514/6.2010-2161>.
- ²³*Digital Time Division Command/Response Multiplex Data Bus*, MIL-STD-1553, US Department of Defense, Washington, DC, Feb. 2018.
- ²⁴C. Whiting and D. Woerner, “Historical RTG performance data through 2020,” data set, *Dryad*, 2023, <https://doi.org/10.5061/dryad.1zcrjdfw2>.



Christopher B. Hersman, Space Exploration Sector, Johns Hopkins University Applied Physics Laboratory, Laurel, MD

Christopher B. Hersman is a systems engineer in APL’s Space Exploration Sector. He has a BS in electrical engineering from the University of Cincinnati and an MS in electronic engineering from Ohio State

University. Chris has over 30 years of aerospace experience and a broad background in many aspects of spacecraft and mission development for scientific and defense applications. He served as the New Horizons spacecraft systems engineer from proposal development through spacecraft launch, after which he was promoted to mission systems engineer. He served in this capacity through both successful flybys and remains in this role today. His email address is chris.hersman@jhuapl.edu.



Gabe D. Rogers, Space Exploration Sector, Johns Hopkins University Applied Physics Laboratory, Laurel, MD

Gabe D. Rogers is the supervisor of APL’s Astrodynamics and Control Systems Group, which is responsible for designing and operating spacecraft guidance and control (G&C) subsystems, mission trajectory

design, and spacecraft navigation. He has a BS and an MS in aeronautical and astronautical engineering from the University of Illinois. Gabe has worked on virtually all of the recent APL space missions in some capacity, from MSX (Midcourse Space Experiment) through Parker Solar Probe, the Double Asteroid Redirection Test (DART), and the Interstellar Mapping and Acceleration Probe (IMAP). He was the lead G&C engineer for the Van Allen Probes mission through integration and test, launch, and the first year of operations. Gabe is the spacecraft systems engineer, deputy mission systems engineer, and G&C lead for the New Horizons mission. His email address is gabe.rogers@jhuapl.edu.



Valerie A. Mallder, Space Exploration Sector, Johns Hopkins University Applied Physics Laboratory, Laurel, MD

Valerie A. Mallder is a flight controller, mission planner, systems engineer, and software engineer in APL’s Space Exploration Sector. She has a BS in computer science from the University of Maryland

University College (now the University of Maryland Global Campus), an MS in computer science from Johns Hopkins University, and an MS in technical management from Johns Hopkins University. Valerie has more than 30 years of experience in systems engineering, full-stack software engineering, leadership, and management, with a broad background in many aspects of spacecraft and space mission development. She is the New Horizons mission flight controller and mission planner. Her email address is valerie.mallder@jhuapl.edu.



Paul E. Rosendall, Space Exploration Sector, Johns Hopkins University Applied Physics Laboratory, Laurel, MD

Paul E. Rosendall is a spacecraft software engineer in APL’s Space Exploration Sector. He has a BS in aerospace engineering from the University of Maryland and an MS in aeronautics and astronautics

from the Massachusetts Institute of Technology (MIT). Paul is the autonomy lead and the command and data handling flight software lead for the New Horizons spacecraft. Paul’s experience includes developing software for deep-space, underwater, and biomedical autonomous systems. His email address is paul.rosendall@jhuapl.edu.



Brian A. Bauer, Space Exploration Sector, Johns Hopkins University Applied Physics Laboratory, Laurel, MD

Brian A. Bauer is a systems engineer in APL's Space Exploration Sector. He has a BS and an MS in aerospace engineering from Washington University in St. Louis and an MS in computer science from Johns

Hopkins University. Brian works on innovative techniques for modeling and simulating the requirements, interfaces, and operations spaces of complex system-of-systems architectures. He was the fault protection/autonomy lead for the New Horizons spacecraft and also worked on various systems engineering projects for high-altitude balloons, hosted payloads, and other mission concepts. Brian teaches the Fundamentals of Space Systems Engineering courses at the Hopkins Whiting School of Engineering. His email address is brian.bauer@jhuapl.edu.



Christopher C. DeBoy, Space Exploration Sector, Johns Hopkins University Applied Physics Laboratory, Laurel, MD

Christopher C. DeBoy is supervisor of the Spaceflight Engineering Branch in APL's Space Exploration Sector. He has a BS from Virginia Polytechnic Institute and State University (Virginia Tech) and an

MS from Johns Hopkins University, both in electrical engineering. His background is principally in line and technical leadership; proposal and program efforts; and spacecraft flight communications systems design, development, and operations. Chris has more than 30 years of experience working on spacecraft communications systems. He designed the command receivers for the TIMED (Thermosphere, Ionosphere, Mesosphere Energetics and Dynamics) and CONTOUR (Comet Nucleus Tour) missions and is the lead telecommunications engineer for the New Horizons mission. His email address is chris.deboy@jhuapl.edu.



Michael A. Vincent, Southwest Research Institute, Boulder, CO

Michael A. Vincent is the director of the Department of Space Operations in the Southwest Research Institute's Solar System Science and Exploration Division. He has BS and MS degrees from the University of Colorado Boulder, both in electrical engineering.

His professional work has primarily been in systems engineering and technical leadership. Michael has more than 20 years of experience working on spacecraft communication systems (New Horizons), payload systems engineering (New Horizons, Lucy), instrument development (Mars Science Laboratory, or MSL), ground system development, and mission operations development (Cyclone Global Navigation Satellite System, or CYGNSS). Most recently, Michael was the mission systems engineer during Step 1 and Phase A for the Lucy mission and is currently the payload systems engineer and encounter phase lead for the Lucy mission. His email is michael.vincent@swri.org.



Richard W. Webbert, Space Exploration Sector, Johns Hopkins University Applied Physics Laboratory, Laurel, MD

Richard W. Webbert is a systems engineer in APL's Space Exploration Sector. He has a BS in electrical engineering from Carnegie-Mellon University and an MS in electrical engineering from Johns Hop-

kins University. Rick has served as lead avionics engineer for a number of components and instruments and as a hardware-design engineer on the MESSENGER (MErcury Surface, Space ENvironment, GEochemistry, and Ranging) integrated electronics module. He worked on the New Horizons power distribution unit and on the autonomy team, where he collaborated closely with systems engineers designing and testing various fault detection and correction algorithms. In addition, Rick served as the Phase E subsystem lead engineer for New Horizons' power system, supporting mission operations, developing subsystem longevity plans, and completing the integration and test of a power system rebuild for the New Horizons operations simulator. His email address is rick.webbert@jhuapl.edu.



Stewart S. Bushman, Space Exploration Sector, Johns Hopkins University Applied Physics Laboratory, Laurel, MD

Stewart S. Bushman is a systems engineer in APL's Space Exploration Sector. He has a BS in mechanical engineering from the University of Rochester and an MS in aeronautical and astronautical engineering

from the University of Illinois Urbana-Champaign. Stewart is the propulsion lead engineer for the New Horizons mission as well as the twin STEREO (Solar TERrestrial Relations Observatory) spacecraft, one of which is still orbiting the Sun, and is also working on the Europa Clipper, IMAP (Interstellar Mapping and Acceleration Probe), and Dragonfly missions. He was formerly the propulsion lead for the MESSENGER (MErcury Surface, Space ENvironment, GEochemistry, and Ranging), Parker Solar Probe, and Van Allen Probes missions. He is a member of the AIAA Liquid Propulsion Technical Committee. His email address is stewart.bushman@jhuapl.edu.



C. Jack Ercol, Space Exploration Sector, Johns Hopkins University Applied Physics Laboratory, Laurel, MD

C. Jack Ercol is a thermal systems engineer in APL's Space Exploration Sector. He has a BS in mechanical engineering from the University of Pittsburgh at Johnstown and an MS in mechanical engineering from the

University of Maryland. Jack previously served as the lead thermal control engineer for NEAR (Near Earth Asteroid Rendezvous) and MESSENGER (MErcury Surface, Space ENvironment, GEochemistry, and Ranging), and he continues as the lead thermal engineer for the New Horizons spacecraft. He was the lead thermal engineer for the Parker Solar Probe thermal control and solar array cooling system during design, fabrication, and testing and is now the lead thermal engineer during flight operations as well as the lead thermal engineer for the

IMAP (Interstellar Mapping and Acceleration Probe) spacecraft. He served as a member of the technical review board for OSIRIS-REx (Origins, Spectral Interpretation, Resource Identification, Security-Regolith Explorer) and is currently one of two non-NASA member of the NESC Thermal Control and Protection Technical Discipline Team. His email address is carl.ercol@jhuapl.edu.



Alice F. Bowman, Space Exploration Sector, Johns Hopkins University Applied Physics Laboratory, Laurel, MD

Alice F. Bowman is the New Horizons mission operations manager in APL's Space Exploration Sector. She has a degree in chemistry and physics from the University of Virginia and has more than 30 years of experience in space operations. In addition to being the mission operations manager for New Horizons, she supervises APL's Space Mission Operations Group, leading approximately 50 staff members who operate deep-space and Earth-orbiting spacecraft, including NASA's TIMED (Thermosphere, Ionosphere, Mesosphere Energetics and Dynamics), STEREO (Solar TERrestrial RELations Observatory), New Horizons, Parker Solar Probe, and, recently, DART (Double Asteroid Redirection Test). Alice's experience also includes national defense space operations, systems engineering, program management, space systems, and space instrument development. Asteroid 146040 Alicebowman, discovered by Marc Buie in 2000, is named after her. She is a member of the Society of Women Engineers, which recently presented her with its prestigious Resnick Challenger Medal, is an AIAA associate fellow, and has served on the International SpaceOps Committee since 2009. Her email address is alice.bowman@jhuapl.edu.



Karl E. Whittenburg, Space Exploration Sector, Johns Hopkins University Applied Physics Laboratory, Laurel, MD

Karl E. Whittenburg is an engineer in APL's Space Exploration Sector. He has a BS in physics from Montclair State University. Karl has 34 years of experience in spacecraft operations and command and control, including supervising the planning and scheduling teams generating command loads for NEAR (Near Earth Asteroid Rendezvous), CONTOUR (Comet Nucleus Tour), MESSENGER (MErcury Surface, Space ENvironment, GEOchemistry, and Ranging), and Parker Solar Probe and mentoring the planning and scheduling lead for New Horizons spacecraft. He has also been a review panel member for various spacecraft flight and ground software design reviews. His email address is karl.whittenburg@jhuapl.edu.



J. Robert Jensen, Space Exploration Sector, Johns Hopkins University Applied Physics Laboratory, Laurel, MD

J. Robert Jensen is an engineer in APL's Space Exploration Sector. He has a BA in chemistry from Cornell College and a PhD in chemistry from the University of Wisconsin-Madison. Bob has extensive experience with radar system design, testing, integration, and performance analysis, as well as experience with satellite communications systems, including aspects that support Doppler and range tracking, and the SPICE library routines to perform precise calculations of spacecraft and planetary body positions in support of the analysis of radiometric tracking data. His email address is bob.jensen@jhuapl.edu.



Steven R. Vernon, Space Exploration Sector, Johns Hopkins University Applied Physics Laboratory, Laurel, MD

Steven R. Vernon is an engineer and supervisor of the Mechanical Systems Group in APL's Space Exploration Sector. He has an AA in engineering science from Howard Community College and a BS in mechanical engineering from Johns Hopkins University. Steven has over 32 years of experience with civilian and military space aerospace industry launch systems, including payload system integration and spacecraft system design, test, assembly, and launch operations. He has led the launch system payload integration and launch campaigns for several missions, including New Horizons. Steven is currently the launch phase lead and deputy chief engineer for Europa Clipper and the National Environmental Policy Act (NEPA) and nuclear launch approval manager for Dragonfly. He has been appointed to consult the NASA Launch Services Program for several launch services acquisitions, is an independent industry consultant for launch systems, and teaches a payload integration course for commercial clients. His email address is steven.vernon@jhuapl.edu.



T. Adrian Hill, Space Exploration Sector, Johns Hopkins University Applied Physics Laboratory, Laurel, MD

T. Adrian Hill is a software engineer in APL's Space Exploration Sector. He has a BS in electrical engineering from the University of Buffalo and an MS in computer science from the Johns Hopkins University. Adrian has over 37 years of experience in real-time embedded software and systems development, with 30 years in flight software and autonomous fault protection for NASA missions. He has held leadership roles on multiple missions and has overseen all phases of the software development process, including requirements definition, design, implementation, and test. Adrian is currently the autonomy lead for the Dragonfly Mission to Titan and supporting autonomy in a lead role for Parker Solar Probe to the Sun. He previously led development of autonomous fault protection systems for Van Allen Probes and New Horizons and led flight software development for MESSENGER (MErcury Surface, Space ENvironment, GEOchemistry, and Ranging). His email address is adrian.hill@jhuapl.edu.



Stephen P. Williams, Space Exploration Sector, Johns Hopkins University Applied Physics Laboratory, Laurel, MD

Stephen P. Williams (retired) was a hardware and software engineer in the Space Exploration Sector. He has a BS in biomedical engineering from Duke, an MS in biomedical engineering from the University of North Carolina, and an MS in electrical engineering from North Carolina State. He developed hardware and software for numerous missions in his 40 years at APL and also served in line management. He was the New Horizons flight software lead during Phases B–D and was the Phase E C&DH subsystem lead until 2021. His email address is atmaintainer6@gmail.com.



Carl S. Engelbrecht, Space Exploration Sector, Johns Hopkins University Applied Physics Laboratory, Laurel, MD

Carl S. Engelbrecht is a propulsion engineer in APL's Space Exploration Sector. He has a BS and an MS in aerospace engineering from the University of Washington. Carl's experience includes line and technical management, with roles such as project manager for the Parker Solar Probe upper stage and dual converter controller

and deputy project manager for Europa Clipper and formerly for New Horizons. He has extensive technical background in the analysis, design, procurement, and integration and test of a wide range of electrical and chemical space propulsion components and systems and knowledge of broad test and launch facilities and their requirements. His email address is carl.engelbrecht@jhuapl.edu.



David Y. Kusnierkiewicz, Space Exploration Sector, Johns Hopkins University Applied Physics Laboratory, Laurel, MD

David Y. Kusnierkiewicz (retired) was chief engineer in APL's Space Exploration Sector. He has a BS and an MS in electrical engineering from the University of Michigan.

Dave has expertise in systems engineering and power system electronics design; design, integration, and test of spaceflight-qualified low-voltage DC/DC converters, high-voltage DC/DC converters, and other power system electronics; and electromagnetic magnetic compatibility issues. He was the mission systems engineer for the New Horizons mission to Pluto and the Kuiper Belt from project inception through launch. He is still the mission systems engineer for the TIMED (Thermosphere, Ionosphere, Mesosphere Energetics and Dynamics) mission. His email address is dave.kusnierkiewicz@jhuapl.edu.